Environmentally Friendly Production of High-Quality and Multifunctional Carbon Quantum Dots (CQD) from Coal

Project #: DE-FE0031997

Presenter: Maohong Fan

Organizations: University of Wyoming
University of Utah

Date: 10/26/2022

U.S. Department of Energy
National Energy Technology Laboratory
Resource Sustainability Project Review Meeting
October 25 - 27, 2022

Project Overview

- Funding: U.S. Department of Energy (DOE)
- Overall Project Performance Dates: 1/1/2020-12/31/2023
- Project Participants:
    - University of Wyoming - Maohong Fan, Dennis N. Coon, Jinke Tang, Zhen Chen, Ramhari Paneru, Ossama Elbanna and Tongtong Wang
    - University of Utah - Eric G. Eddings and Alex Prlina

Project objectives and goals

Objectives:

- Developing an innovative, simple, low-temperature, cost-effective, environmentally friendly technology for producing high-value coal-derived quantum dots (CQDs)
- Evaluating the applications of the CQDs in solar cell for clean energy production and photocatalysis for clean air and health protection.

Goals:

- Technically - Preparing coal-derived CQDs with
  - Carbon in CQDs: 100% from coal
  - Diameters: 2 -7 nm
  - Purity: >99%
- Environmentally
  - Wastewater discharge: near-zero
  - Air pollution: near-zero (near 100%-purity CO_2 is produced and directly captured)
- Economically
  - The profit: >50% (based on 10,000-ton/year production scale and $30,000/ton-CQD)

Background

- Conventional coal utilization – combustion
  - Generation of huge amount of flue gas containing low concentration of CO_2
  - Capture of the CO_2 is expensive
  - Thus, low carbon emission utilization methods are needed
- Why coal to carbon materials?
  - Carbon materials need C-rich feedstocks
  - Coals are well known C-rich materials, thus are great candidates for carbon materials
  - Economically, the values of coal derived carbon materials > values of coal derived fuels
  - Environmentally, the carbon footprints of coal derived carbon materials < footprints of coal derived fuels
- Why did we propose this project?
  - CQD is a carbon material
  - The proposed coal based CQD production technology has the following advantages
    - Simple

Technical Approach

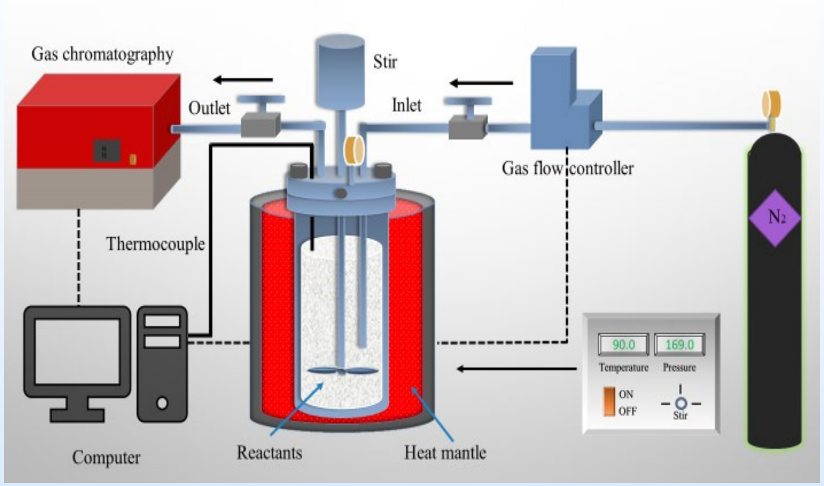

Figure 1. Schematic diagram of the experimental setup for the synthesis of the CQDs production from coal and H_2O_2.

- Materials: 10 g dried coal, and 1.5 L H_2O_2 solution were added into a Parr 2526 high-pressure reactor. The reactor was purged by N_2, and the starting pressure was atmosphere pressure. Gas, liquid and solid products were collected.
- Reaction temperatures: 60, 70, 80, 90, and 100 ^oC.
- Reaction times: 2, 4, 6, 8, 10, and 12 hours.
- H_2O_2 concentrations:1.5%, 2.0%, 2.5%, 3.0% and 3.5%.

Effect of H_2O_2 concentration

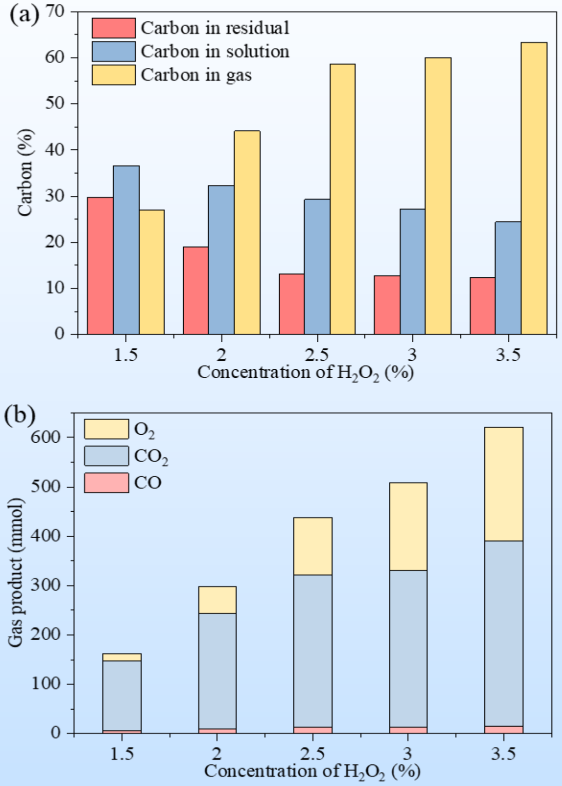

Figure 2. (a) Carbon distribution in the final products (gas, solution, and residual); (b) Gas products and their distributions, resulting from the reactions with different H_2O_2 concentrations (1.5%-3.5%) at 90 ^{o}C for 12 hrs.

- (**a**): In general, the increase in H_2O_2 concentration leads to the increase in carbon in the gas portion but the decreases in carbons in residual and solution portions.
- (**b**): In general, H_2O_2 concentration increase leads to the increase in the increase in CO_2 in gas portion.
- (a) And (b) indicated higher H_2O_2 concentration promoted oxidation.

Effect of H_2O_2 concentration (continued)

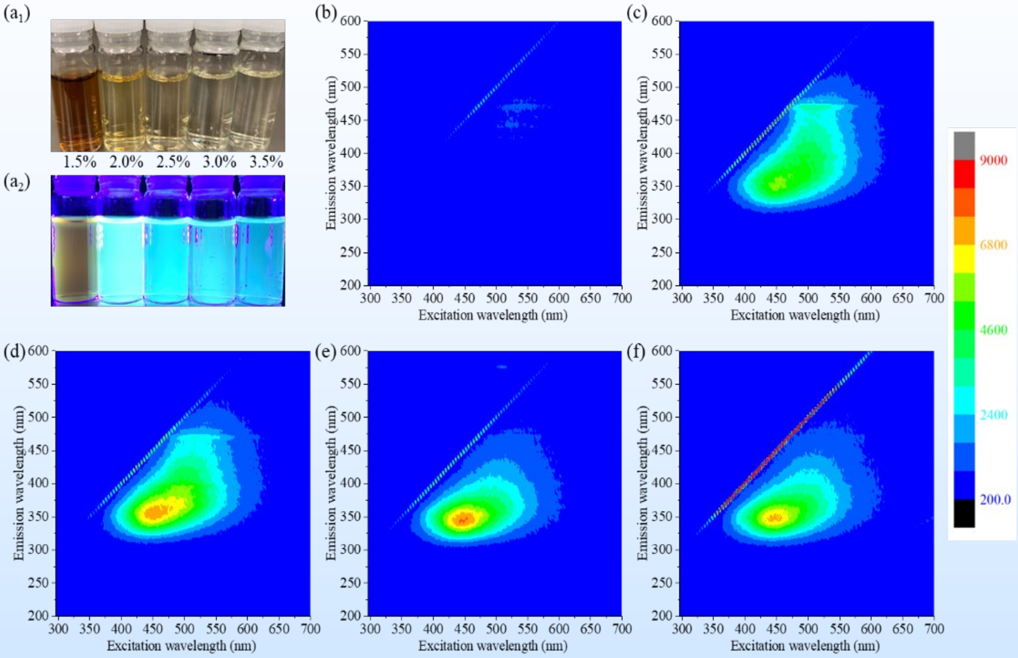

- Figure 1 (b) – (e): photoluminescence effect increases as the H_2O_2 concentration increases.
- Figure 1 (f): The lower photoluminescence effect of 3.5% H_2O_2 compared to that of 3.0% (e) might be due to the destruction of some aromatic structures as a result of excessive concentration of H_2O_2 [1].
- Figure 2: The increase in the concentration of H_2O_2 leads to the decrease in the absorption wavelength and thus increase in the energy gap between ground state and excited state of CQD molecules.

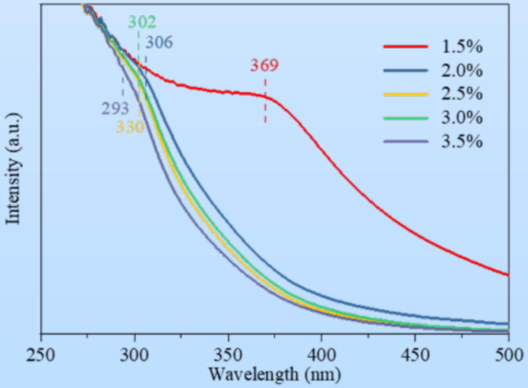

Figure 1 (upper). Photos (a1 and a2) and fluorescence spectra (b-f) of CQDs-containing solutions obtained with different H_2O_2 concentrations (1.5%-3.5%) at 90 ^{o}C for 12 hrs: (a_1) in daylight, (a_2 under 365-nm UV excitation, (b)1.5%, (c) 2.0%, (d) 2.5%, (e) 3.0%, and (f) 3.5%.
Figure 2 (left). UV spectra of CQDs-containing solutions from the reactions at different H_2O_2 concentrations (1.5%-3.5%) at 90 ^{o}C for 12 hours.

Effect of temperatures

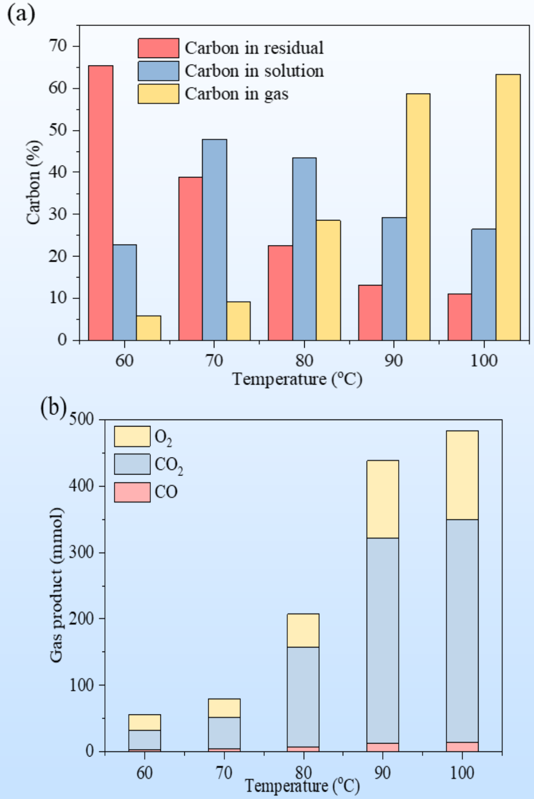

Figure 1. (a) Carbon distributions in the final products (gas, solution, and residual); (b) gas products and their distributions, resulting from the reactions at different temperatures (60-100 °C) with 2.5% H_2O_2 for 12 hrs.

- (a): as reaction temperature increased, the carbon in the gas increased, but that in residual decreased.
- (b): as H_2O_2 concentration increased, the product of O_2 CO_2 and CO increased.
- (a) And (b) indicated higher temperature enhanced scission of the chemical bonds in organic compounds of coal undergoing decomposition [2].

Effect of temperatures (continued)

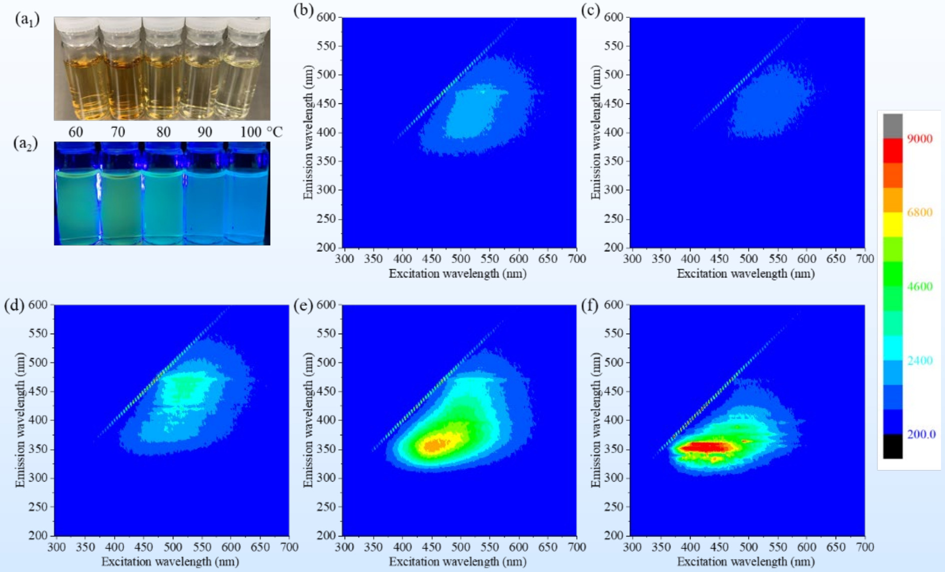

- Figure 1 (b) – (e): The higher the reaction temperature, the stronger the photoluminescence effect. This was attributed to the greater CQD concentrations.

- Figure 2: In general, the increase in reaction temperature leads to the decrease in the absorption wavelength and thus increase in the energy gap between ground state and excited state of CQD molecules [3].

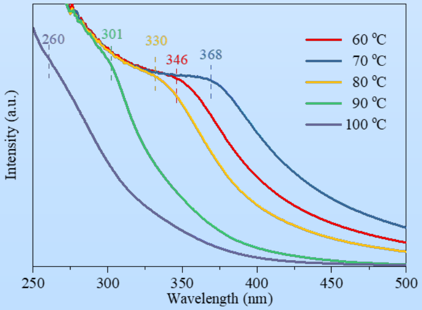

Figure 1 (upper). Photos and fluorescence spectra images of CQDs-containing solutions from the reactions at different temperatures (60-100 °C) with 2.5% H_2O_2 for 12 hours: (a1) in daylight, (a2) under 365-nm UV excitation, (b) 60 °C, (c) 70 °C, (d) 80 °C, (e) 90 °C, and (f) 100 °C.

Figure 2 (left). UV spectra of CQDs-containing solutions from the reactions at different temperatures (60-100 °C) with 2.5% H_2O_2 for 12 hours.

Effect of reaction time

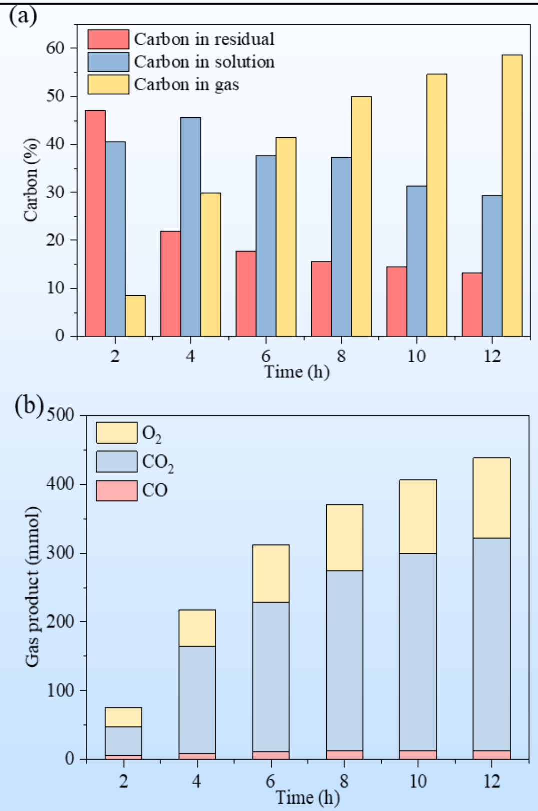

Figure 8. (a) Carbon distribution in the final products (gas, solution, and residual); (b) Gas products and their distributions, resulting from the reactions at different reaction times (2-12 hr) with 2.5% H_2O_2 at 90 ^{o}C.

- (a): As reaction time increased, the carbon in the gas increased, and that in the residual decreased.
- (b): Longer reaction time increased the yield of O_2, CO_2 and CO gases.
- (a) and (b) indicated longer reaction time pronounced the reaction.

Effect of reaction time (continued)

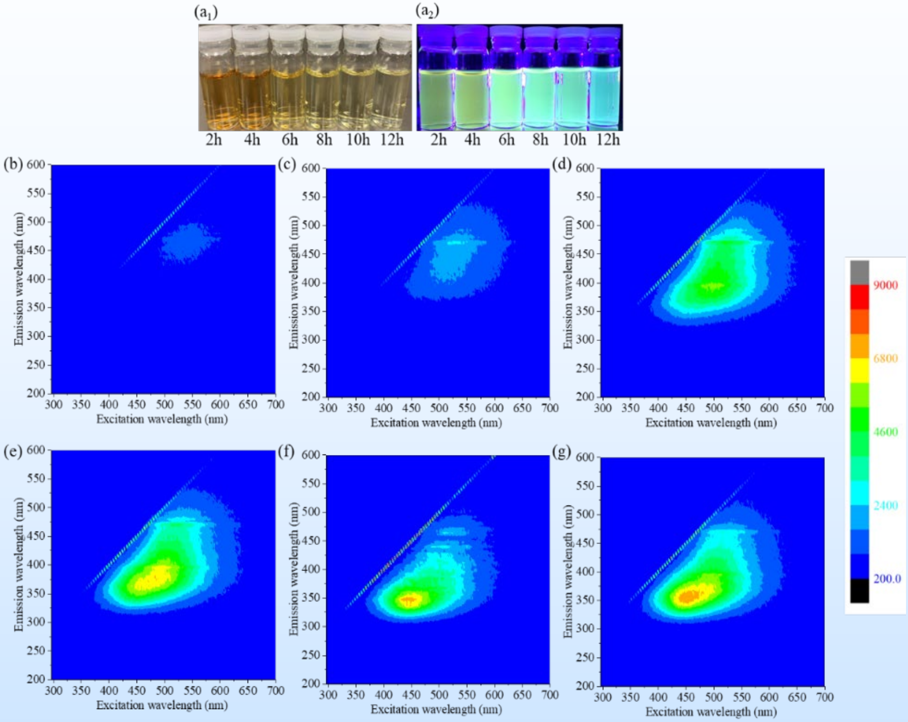

- Figure 1 (b) – (g): the longer the reaction time, the higher intensity of the photoluminescence effect.

- Figure 2: as the reaction time increased, the absorption shoulder on the UV-vis shifted towards lower wavelength.

- Figure 1 and 2 indicated that smaller size CQDs were produced when the reaction time was longer.

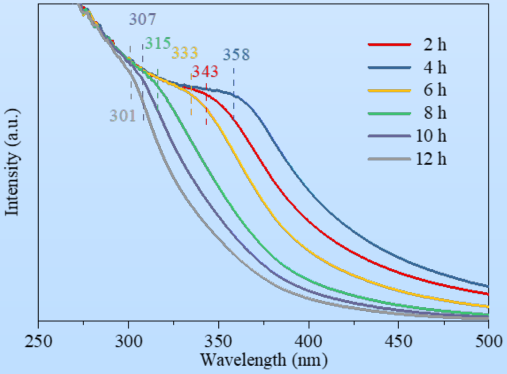

Figure 1 (upper). Photos (a$_1$ and a$_2$) and fluorescence spectra (b-f) of CQDs-containing solutions from the reactions at different reaction times (2-12 hr) with 2.5% H_2O_2 at 90 ^{o}C: (a$_1$) in daylight, (a$_2$) under 365-nm UV excitation, (b) 2 hr, (c) 4 hr, (d) 6 hr, (e) 8 hr, (f) 10 hr, and (g) 12 hr.

Figure 2 (left): UV spectra images of CQDs-containing solutions from the reactions at different reaction times (2-12 hr) with 2.5% H_2O_2 at 90 ^{o}C.

Effect of in-situ Fenton reaction

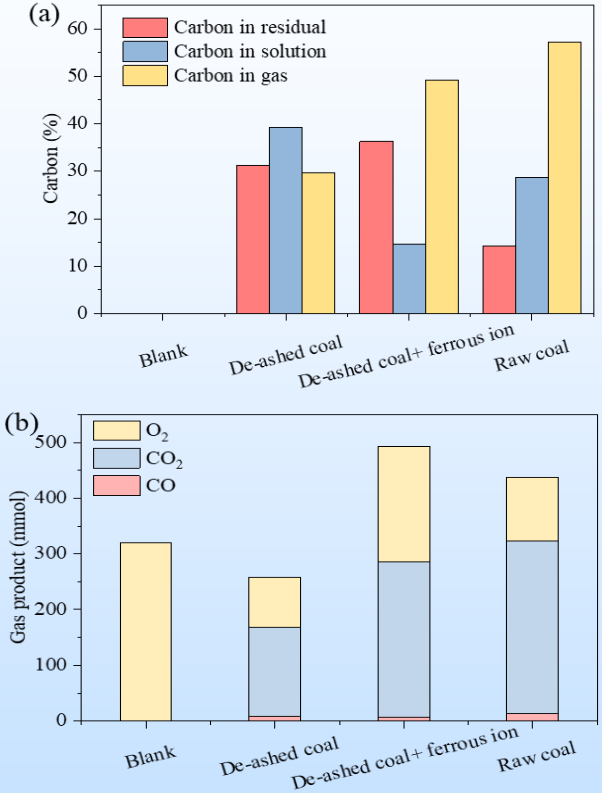

Figure 1. (a) Carbon distribution in the final products (gas, solution, and residual); (b) Gas products and their distributions, resulting from different raw materials (blank, de-ash coal, de-ash coal + 30 ppm Fe^{2+}, and raw coal) at 90 ^{o}C with 2.5% H_2O_2 for 12 hours.

- (a): the percentages of carbon in gas were higher when raw coal and deashed coal + ferrous ion was used, compared to blank and when only deashed coal was used.
- (b): when deashed coal + ferrous ion was used, the amount of O_2 in the gas product was higher than when raw coal was used, but the amount of CO plus CO_2 was lower. When only deashed coal was used, the amount of O_2 and CO_2 was the lowest.
- (a) and (b) indicated ferrous ion accelerated H_2O_2 decomposition into O_2 and H_2O, and ferrous ion in raw coal can promote the reaction more efficiently.

Study on the catalytic effect of Fe^{2+} in coal on CQD formation

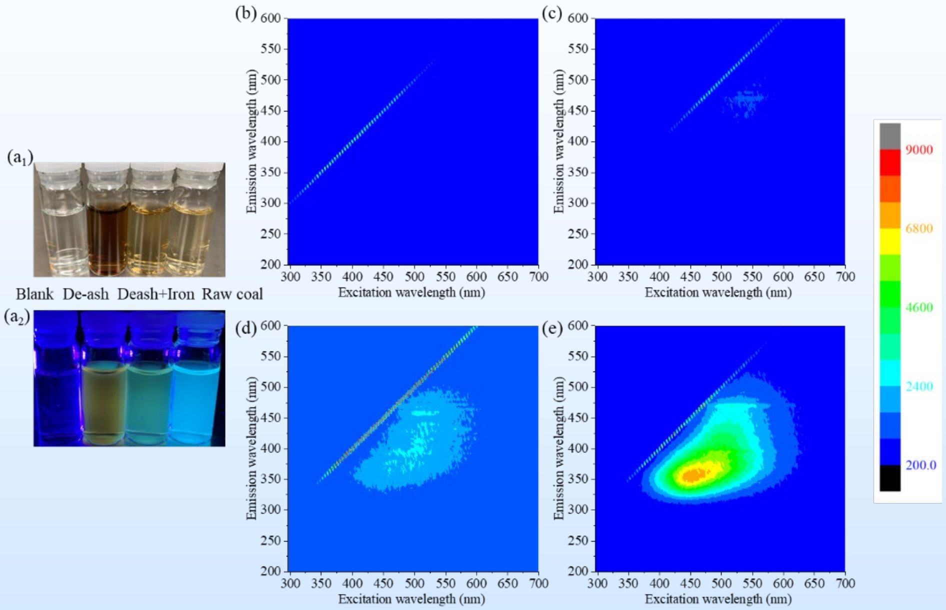

- Figure 1 (e): the photoluminescent effect was the strongest when raw coal was used.
- Figure 2: when raw coal was used, CQD abortion shoulder was at 301 nm, lower than 311 nm when de-ash coal and 30 ppm Fe^{2+} was used. This indicated a smaller size CQDs when raw coal was used.
- In de-ash coal + ferrous ions, ferrous ions were added, but when raw coal was used, ferrous ions were gradually released. The graduate release could more effectively promote Fenton reaction and reduce formation of O_2.

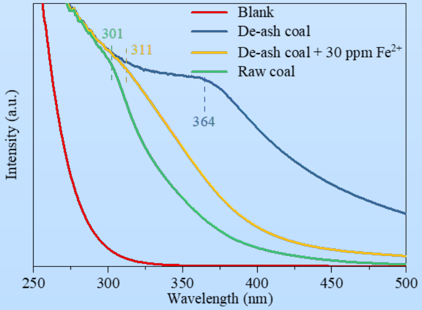

Figure 1 (upper): (a) Photos and fluorescence spectra of CQDs, resulting from different raw materials (blank, de-ash coal, de-ash coal + 30 ppm Fe^{2+}, and raw coal) at 90 ^{o}C with 2.5% H_2O_2 for 12 hours.

Figure 2 (left): UV spectra of CQDs-containing solutions for different raw materials (blank, de-ash coal, de-ash coal + 30 ppm Fe^{2+}, and raw coal) at 90 ^{o}C with 2.5% H_2O_2 for 12 hours.

Transmission electron microscopy (TEM) images of CQDs

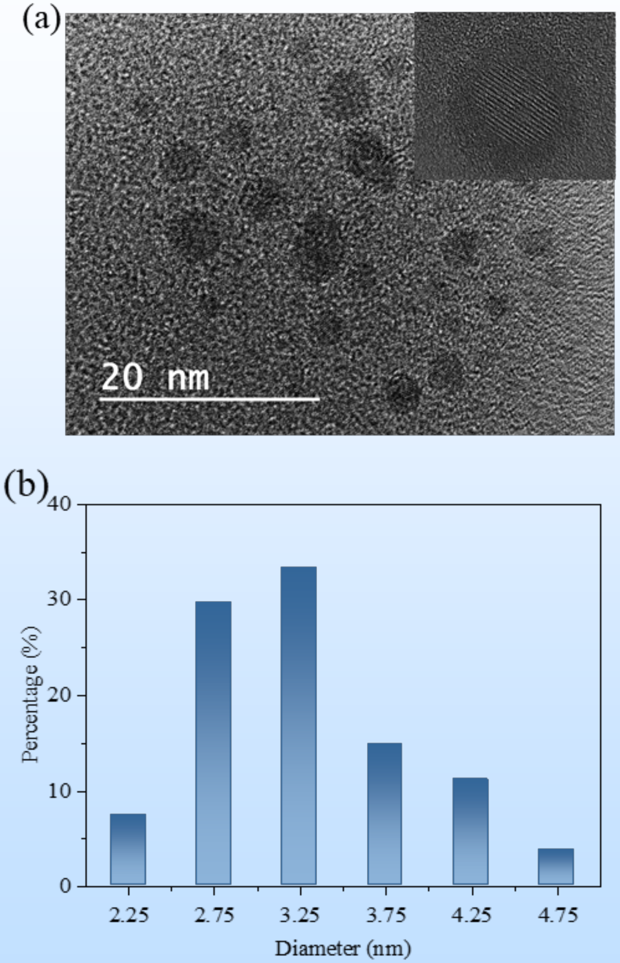

Figure 1 - The TEM image and diameter distributions of the CQDs synthesized from raw coal with 2.5% H_2O_2 at 90 ^{o}C for 12 h.

- (a): The CQDs are spherical and mono-dispersive within the solution.

- (b): Based on the statistical analysis of their TEM images, the particle sizes of the CQDs are in the range of 2-5 nm, with an average size of ~3 nm.

Study on the catalytic effect of Fe^{2+} in coal on CQD formation

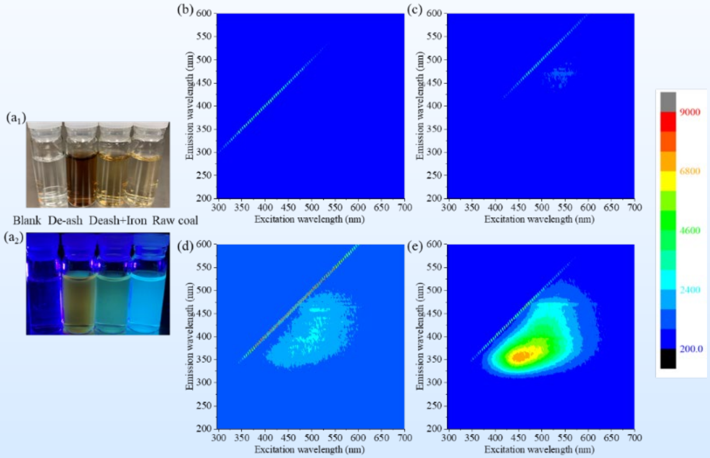

- Figure 1 (e): the photoluminescent effect is the strongest when raw coal is used.
- Figure 2: when raw coal is used, CQD abortion shoulder is at 301 nm, lower than 311 nm when de-ash coal and 30 ppm Fe^{2+} is used, indicating the formation of smaller-size CQDs when raw coal is used.
- In de-ash coal + ferrous ions, ferrous ions are added, but when raw coal is used, ferrous ions are gradually released. The graduate release could more effectively promote Fenton reaction and reduce formation of O_2.

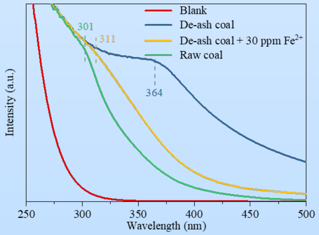

Figure 1 (upper): Photos and fluorescence spectra images of CQDs-containing solutions from different raw materials (blank, de-ash coal, de-ash coal + 30 ppm Fe^{2+}, and raw coal) at 90 ^{o}C with 2.5% H_2O_2 for 12 hrs: (a1) in daylight, (a2) under 365-nm UV excitation, (b) blank (H_2O_2) , (c) de-ash coal, (d) de-ash coal + 30 ppm Fe^{2+}, and (e) raw coal.

Figure 2 (left): UV spectra of CQDs-containing solutions for different raw materials (blank, de-ash coal, de-ash coal + 30 ppm Fe^{2+}, and raw coal) at 90 ^{o}C with 2.5% H_2O_2 for 12 hours.

Kinetics

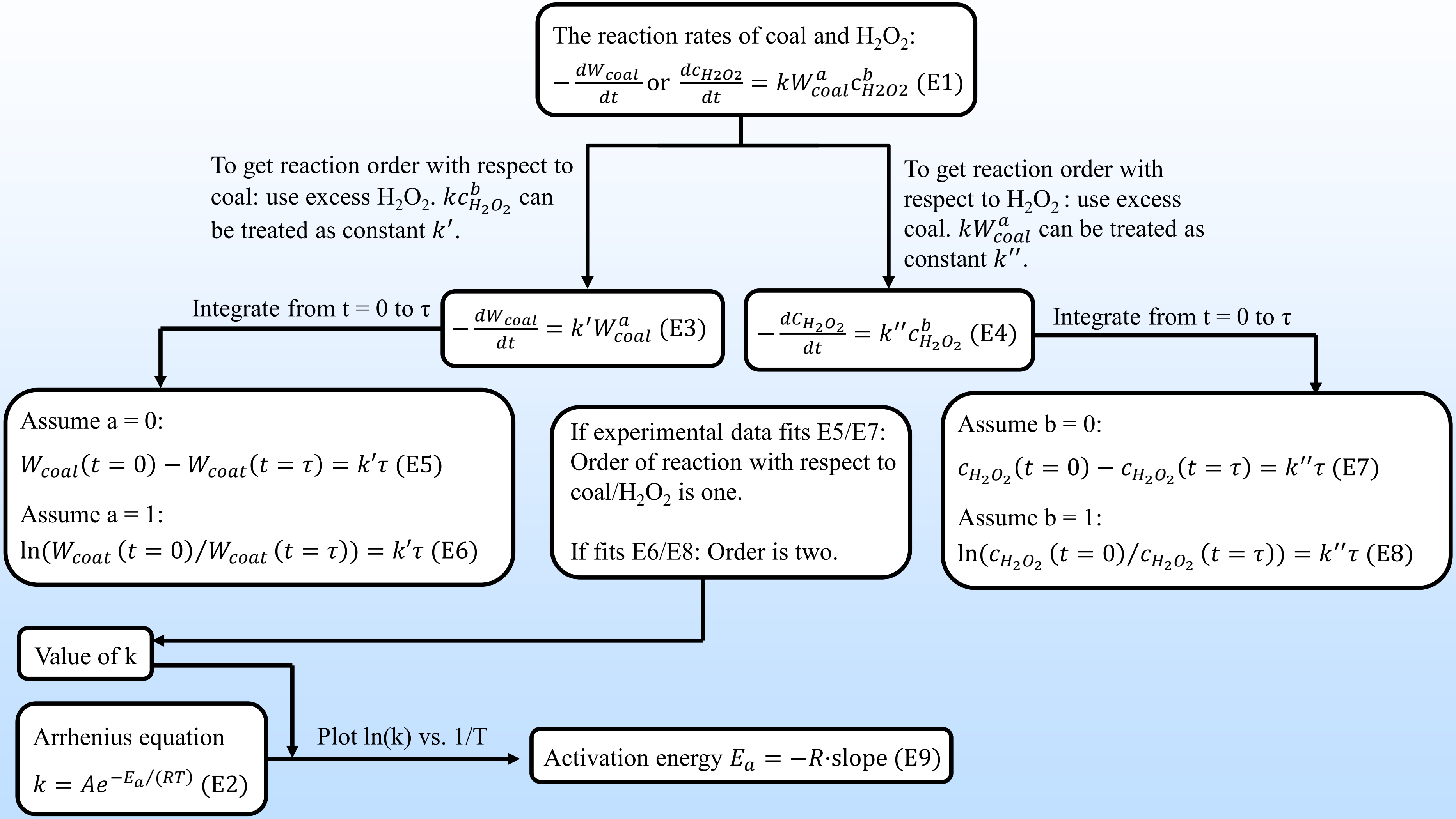

The reaction rates of coal and H_2O_2:

$$-\frac{dW_{coal}}{dt} \text{ or } \frac{dc_{H2O2}}{dt} = kW_{coal}^{a}c_{H2O2}^{b} \text{ (E1)}$$

To get reaction order with respect to coal: use excess H_2O_2. $kc_{H_2O_2}^{b}$ can be treated as constant k'.

To get reaction order with respect to H_2O_2 : use excess coal. kW_{coal}^{a} can be treated as constant k''.

$$-\frac{dW_{coal}}{dt} = k'W_{coal}^{a} \text{ (E3)}$$

$$-\frac{dC_{H_2O_2}}{dt} = k''c_{H_2O_2}^{b} \text{ (E4)}$$

Integrate from t = 0 to τ

Assume a = 0:

$$W_{coal}(t=0) - W_{coat}(t=\tau) = k'\tau \text{ (E5)}$$

Assume a = 1:

$$\ln(W_{coat}(t=0)/W_{coat}(t=\tau)) = k'\tau \text{ (E6)}$$

Integrate from t = 0 to τ

Assume b = 0:

$$c_{H_2O_2}(t=0) - c_{H_2O_2}(t=\tau) = k''\tau \text{ (E7)}$$

Assume b = 1:

$$\ln(c_{H_2O_2}(t=0)/c_{H_2O_2}(t=\tau)) = k''\tau \text{ (E8)}$$

If experimental data fits E5/E7: Order of reaction with respect to coal/H_2O_2 is one.

If fits E6/E8: Order is two.

Value of k

Arrhenius equation

$$k = Ae^{-E_a/(RT)} \text{ (E2)}$$

Plot ln(k) vs. 1/T

Activation energy $E_a = -R\cdot$slope (E9)

where W_{coal} is the concentration (g/mL) of coal in the reaction, $C_{H_2O_2}$ is the concentration (g/mL) of H_2O_2 in the reaction, k is the reaction rate constant, t is the reaction time, a is the reaction order of H_2O_2, and b is the reaction order of coal, A (s^{-1}) is the Arrhenius pre-exponential factor for the reaction, E_a (J/g, or J/mol) is the activation energy for the reaction of coal and H_2O_2, R ($J\ g^{-1}K^{-1}$ or $J\ mol^{-1}K^{-1}$) is the universal gas constant, T (K) is the absolute temperature of the reaction.

Techno-economical analysis and environmental impacts of coal to CQDs technology

ASPEN Plus version 12 was used to simulate the process

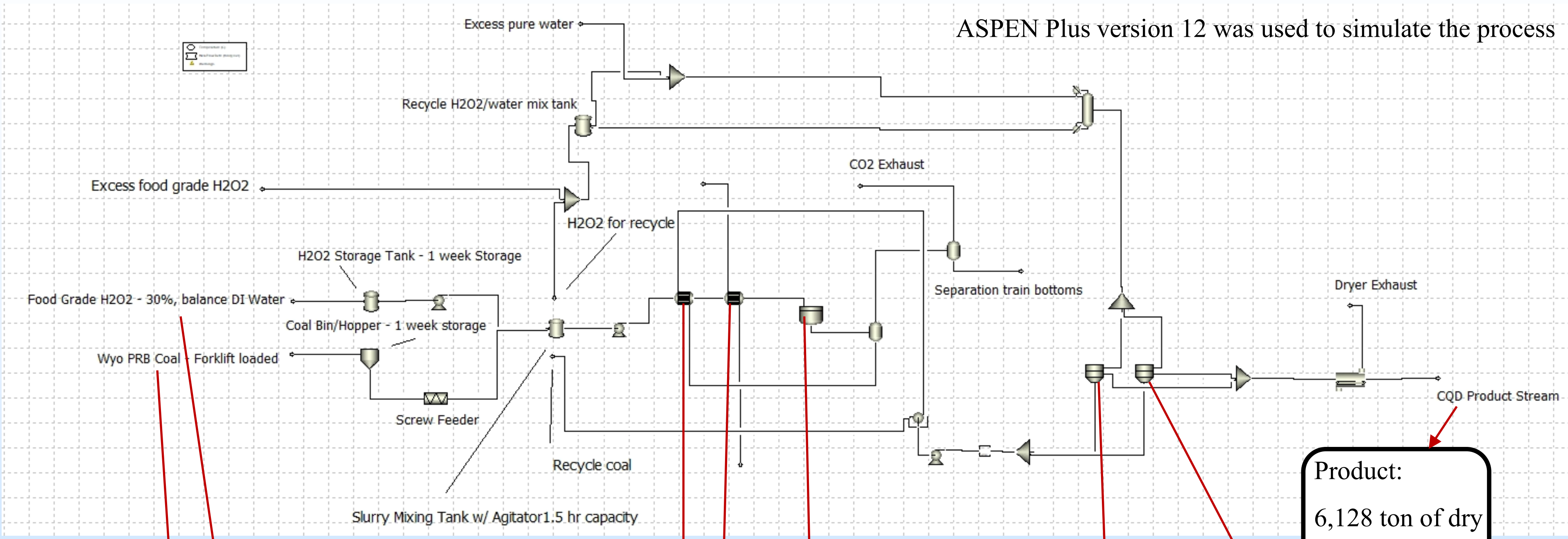

Feed:

25,000 tons per year of Wyoming Powder River Basin (PRB) coal (specified in the original project narrative);

1.043×10^6 tons per year 30 wt% H_2O_2 solution (food grade). The coal/H_2O_2 solution ratio is 1:41, consistent with the experiments.

Shell and tube heat exchangers to heat the reactants to 90 °C

The mixture is held 90 °C and stirred for 12 h in hydrothermal reactor.

Continuous-scroll, solid-bowl centrifuges where CQDs are separated from H_2O_2 solution

Product:

6,128 ton of dry CQDs per year.

Summary Slide

- The major factors affecting CQDs synthesis with coal have been identified
- How each factor affects CQDs synthesis is understood, and the optimal conditions have been obtained
- Good-quality CQDs have been successfully synthesized with coal via Fenton reaction
- Reaction kinetics of the coal-derived CQDs synthesis has been established
  - Reaction orders
  - Activation energy
- The catalytic effect of Fe^{2+} in coal on CQDs synthesis has been confirmed with experiments
- The application of the CQDs in solar cell has been studied
- Techno-economical analysis is being conducted.

Appendix

- These slides will not be discussed during the presentation but are mandatory.

Order of reaction

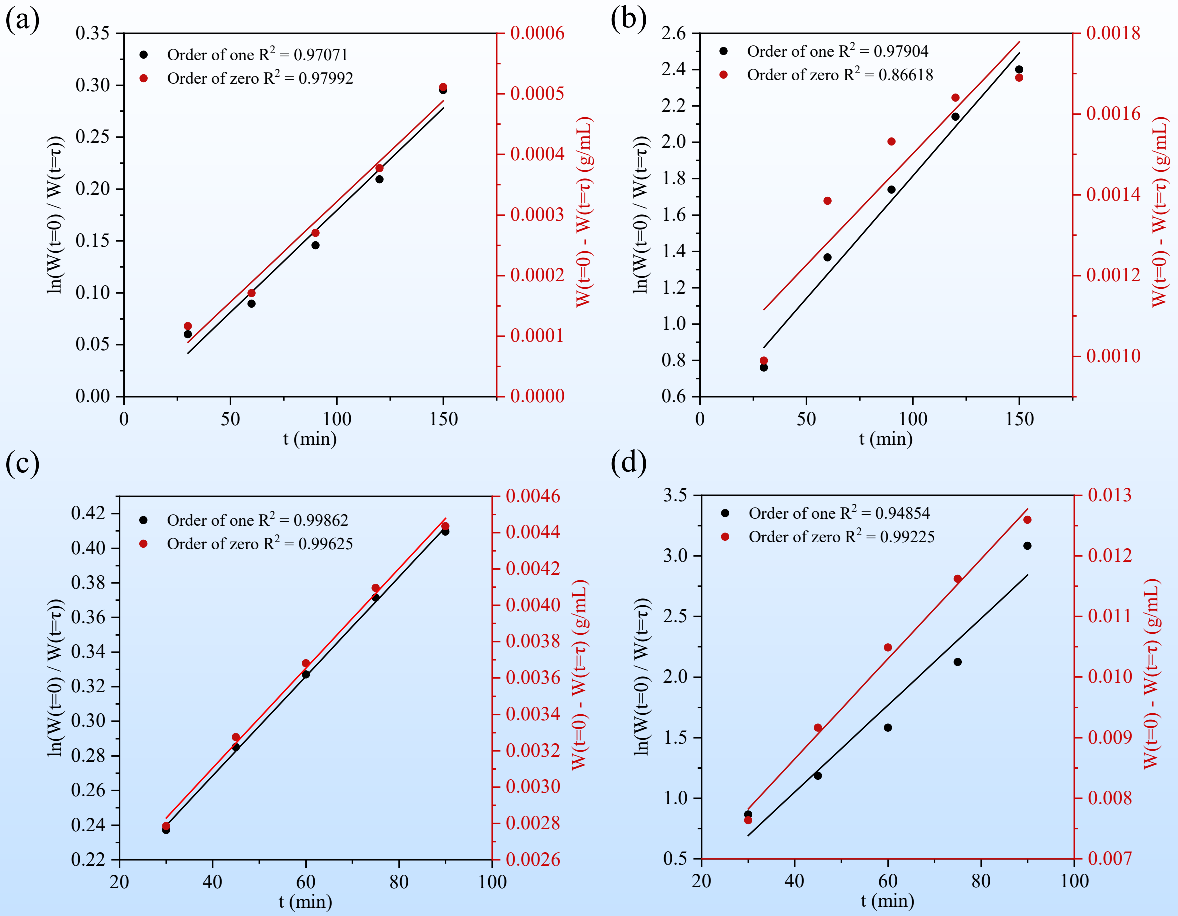

Figure 17. Concentration vs. time plot to determine the order of reaction with respect to (a) de-ash coal, (c) H_2O_2 reacting with de-ash coal, (b) raw coal, (d) H_2O_2 reacting with raw coal.

- (a) and (b): according to the value of R^2, it was challenging to determine the order of reaction with respect to de-ash coal and that of H_2O_2.

- (c) and (d): when raw coal reacted with H_2O_2, the order of reaction with respect to raw coal was one, and that of H_2O_2 was zero.

Activation energy

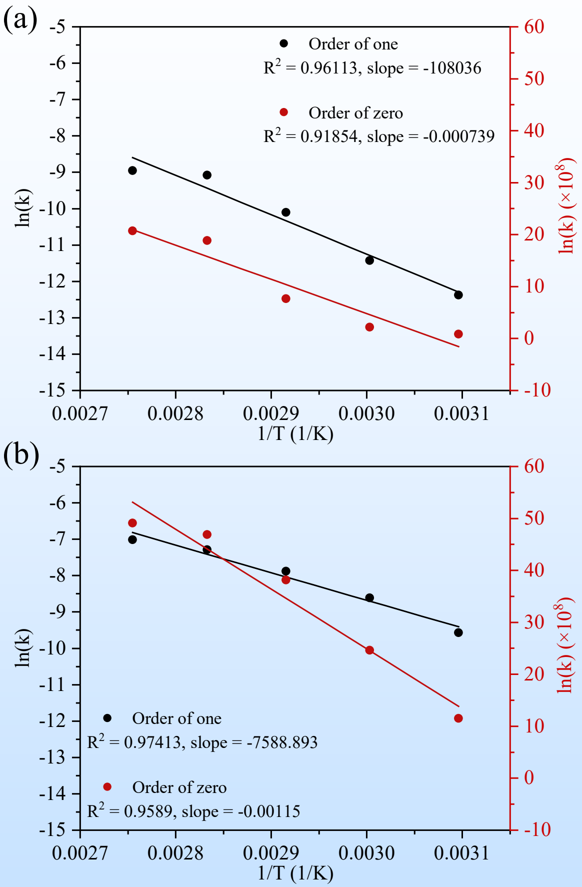

Figure 18. Concentration vs. time plot to determine the order of reaction with respect to (a) de-ash coal, (c) H_2O_2 reacting with de-ash coal, (b) raw coal, (d) H_2O_2 reacting with raw coal.

- The activation energy was studied using excessive H_2O_2.
- (a): With higher R^2, order of reaction with respect to de-ash coal was one. According to eq E9, the activation energy was Ea(de-ash coal) = 7507.542 J/g.
- (b): The result corroborated with Figure 17 (d), that the order of reaction with respect to raw coal was one. The activation energy was Ea(raw coal) = 5257.84 J/g.
- With ash in the coal, the activation energy was lower than when there was no ash, this proved that the ash catalyzed the reaction to produce CQDs.

Free on board and bare module costs

Equipment costing was performed for the once-through process according to the Guthrie method described in Seider et. al [7].

Table 1. Free on board and bare module costs for coal-CQD process equipment

Equipment Type	f.o.b. Purchase Cost ($) CEPCI = 806.9	Bare Module Factor	Bare Module Cost ($)
Electric Motors	2,686	3.3	8,865
Centrifugal Pumps	596,193	3.3	1,967,438
Shell and Tube Heat Exchangers	270,380	3.17	857,105
Pressure Vessels	274,394	4.16	836,376
Trayed Columns	601,673	4.16	2,502,959
Rotary Drum Vacuum Filters	186,622	2.32	616,152
Centrifuges	353,339	2.03	717,278
Batch Tray Driers	26,090	2.06	53,746
Storage and Mixing Tanks	1,985,681	N/A	1,985,681
Hoppers	66,226	N/A	66,226
Agitators	561,687	N/A	561,687
Forklifts	32,500	N/A	32,500
Total	4,957,471		12,765,014

Future work

- Continue to evaluation of the photoelectric performances of CQDs (i.e., application in solar cell)   (Task 4)
- Continue to evaluate the performances of CQDs in modifying photocatalyst   (Task 5)
- Continue to work on techno-economic analysis (Task 7)
  - Integration of cycle and heat streams
  - Optimizing the whole production process
  - Calculating profitability
- Scale-up CQDs production (not a task of this project)

Organization Chart

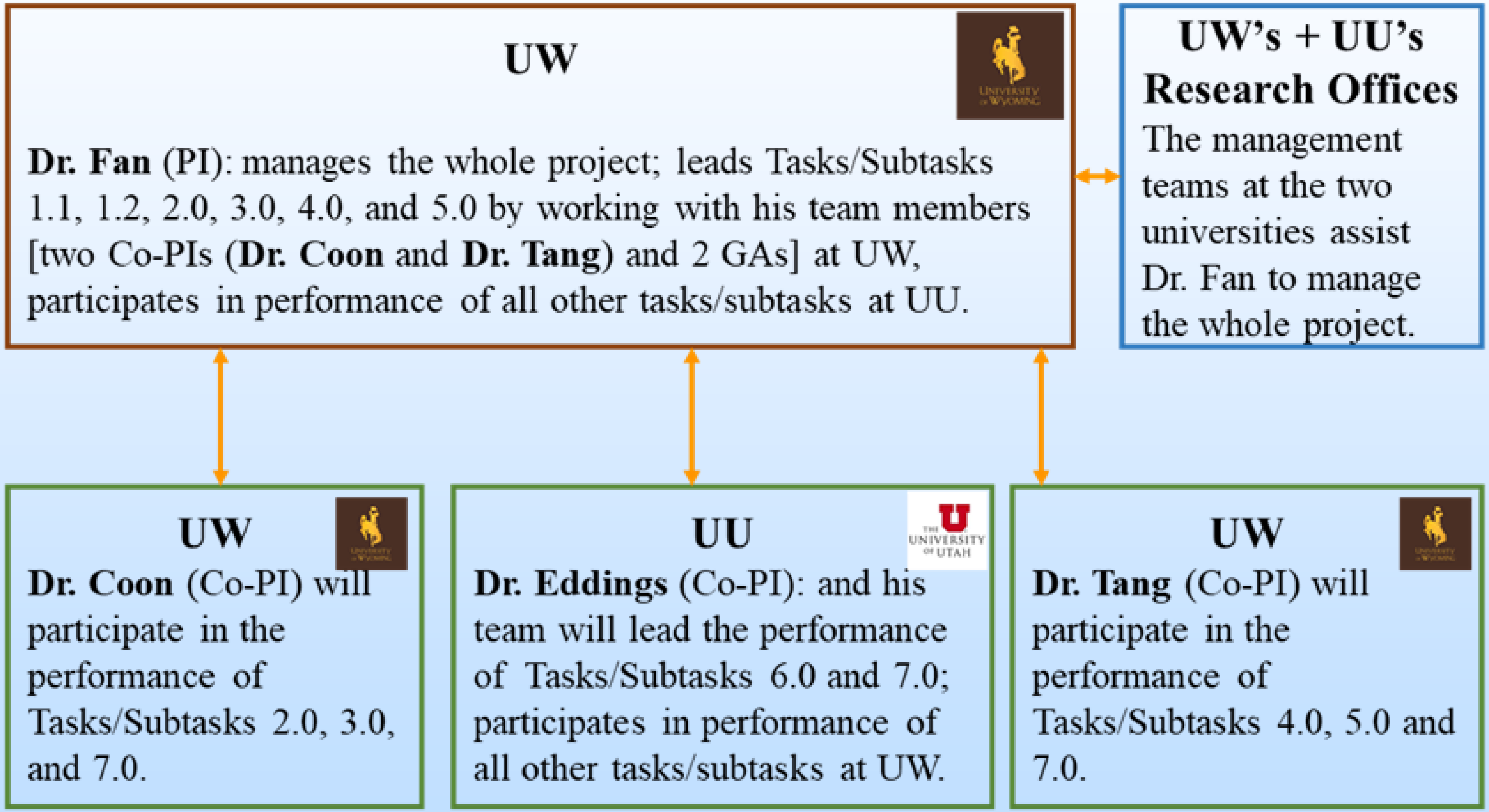

UW

Dr. Fan (PI): manages the whole project; leads Tasks/Subtasks 1.1, 1.2, 2.0, 3.0, 4.0, and 5.0 by working with his team members [two Co-PIs (**Dr. Coon** and **Dr. Tang**) and 2 GAs] at UW, participates in performance of all other tasks/subtasks at UU.

UW's + UU's Research Offices

The management teams at the two universities assist Dr. Fan to manage the whole project.

UW

Dr. Coon (Co-PI) will participate in the performance of Tasks/Subtasks 2.0, 3.0, and 7.0.

UU

Dr. Eddings (Co-PI): and his team will lead the performance of Tasks/Subtasks 6.0 and 7.0; participates in performance of all other tasks/subtasks at UW.

UW

Dr. Tang (Co-PI) will participate in the performance of Tasks/Subtasks 4.0, 5.0 and 7.0.

(UW: University of Wyoming; UU: University of Utah; GA: graduate assistant)

Gantt Chart

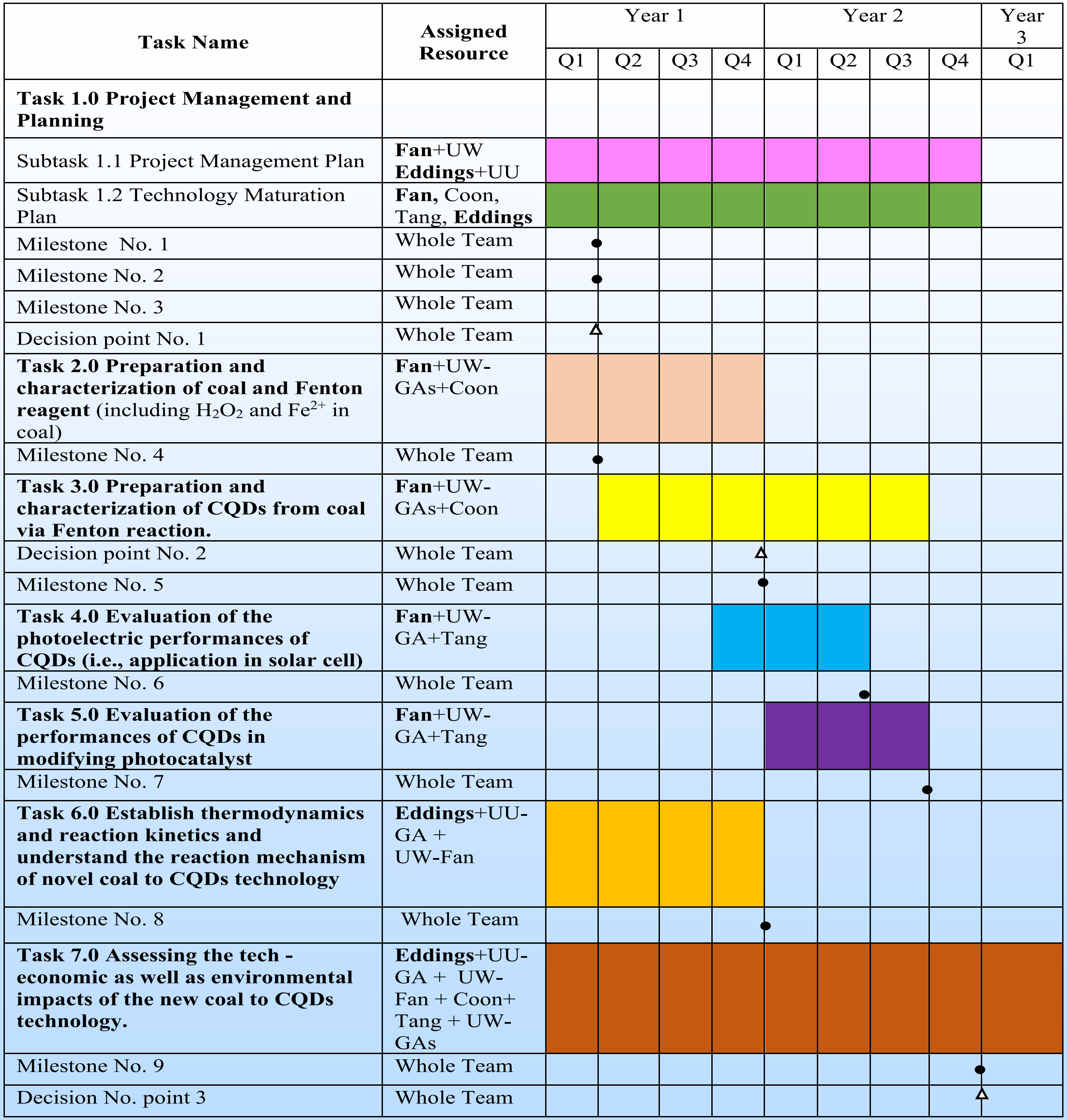

Task Name	Assigned Resource	Year 1				Year 2				Year 3
		Q1	Q2	Q3	Q4	Q1	Q2	Q3	Q4	Q1
Task 1.0 Project Management and Planning										
Subtask 1.1 Project Management Plan	**Fan**+UW **Eddings**+UU	■	■	■	■	■	■	■	■	
Subtask 1.2 Technology Maturation Plan	**Fan,** Coon, Tang, **Eddings**	■	■	■	■	■	■	■	■	
Milestone No. 1	Whole Team	●								
Milestone No. 2	Whole Team	●								
Milestone No. 3	Whole Team									
Decision point No. 1	Whole Team	△								
Task 2.0 Preparation and characterization of coal and Fenton reagent (including H_2O_2 and Fe^{2+} in coal)	**Fan**+UW-GAs+Coon	■	■	■	■					
Milestone No. 4	Whole Team	●								
Task 3.0 Preparation and characterization of CQDs from coal via Fenton reaction.	**Fan**+UW-GAs+Coon		■	■	■	■	■	■		
Decision point No. 2	Whole Team				△					
Milestone No. 5	Whole Team				●					
Task 4.0 Evaluation of the photoelectric performances of CQDs (i.e., application in solar cell)	**Fan**+UW-GA+Tang				■	■	■			
Milestone No. 6	Whole Team						●			
Task 5.0 Evaluation of the performances of CQDs in modifying photocatalyst	**Fan**+UW-GA+Tang					■	■	■		
Milestone No. 7	Whole Team							●		
Task 6.0 Establish thermodynamics and reaction kinetics and understand the reaction mechanism of novel coal to CQDs technology	**Eddings**+UU-GA + UW-Fan	■	■	■	■					
Milestone No. 8	Whole Team				●					
Task 7.0 Assessing the tech -economic as well as environmental impacts of the new coal to CQDs technology.	**Eddings**+UU-GA + UW-Fan + Coon+ Tang + UW-GAs	■	■	■	■	■	■	■	■	■
Milestone No. 9	Whole Team								●	
Decision No. point 3	Whole Team								△	

References

- [1] Science Abstracts, London: E. & F.N. Spon, 1919.
- [2] W. Ning, X. Donghai, H. Botian, G. Shuwei, G. Yang and W. Shuzhong, "Chemical reactions of organic compounds in supercritical water gasification and oxidation," Water Research, vol. 190, 2021.
- [3] B. Anusuya, S. Monikankana, D. Tonkeswar, G. Rajib Lochan and S. Binoy K., "Blue-emitting fluorescent carbon quantum dots from waste biomass sources and their application in fluoride ion detection in water," Journal of Photochemistry & Photobiology, B: Biology, vol. 209, 2020.
- [4] S. Arumugam Selva, X. Jing, V. Annavaram and R. Yawen, "Facile preparation of fluorescent carbon quantum dots from denatured sour milk and its multifunctional applications in the fluorometric determination of gold ions, in vitro bioimaging and fluorescent polymer film," Journal of Photochemistry and Photobiology A: Chemistry, vol. 401, 2020.
- [5] S. Monikankana, H. James C., D. Tonkeswar, D. Trisharani and S. Binoy K., "Feasibility study of preparation of carbon quantum dots from Pennsylvania anthracite and Kentucky bituminous coals," Fuel, vol. 243, pp. 433-440, 2019.
- [6] D. Akansha, U. Takashi, M. Toru and T. Masaru, "Synthesis and characterization of Mono-disperse Carbon Quantum Dots from Fennel Seeds: Photoluminescence analysis using Machine Learning," vol. 9, 2019.
- [7] W. e. Seider, Product and Process Design Principles: Synthesis, analysis and Evaluation, 4 ed., 2017.

Thank DOE program managers for their guidance!

Thank you!